ARTICLE

Notch3-regulated microRNAs impair CXCR4-dependent maturation of thymocytes allowing maintenance and progression of T-ALL

Ilaria Sergio[1,13], Claudia Varricchio[2,13], Sandesh Kumar Patel[2,13], Martina Del Gaizo[3], Eleonora Russo[2], Andrea Orlando[4], Giovanna Peruzzi[5], Francesca Ferrandino[6], Georgia Tsaouli[7], Sonia Coni[2], Daniele Peluso[8], Zein Mersini Besharat[1], Federica Campolo[1], Mary Anna Venneri[1], Donatella Del Bufalo[9], Silvia Lai[3], Stefano Indraccolo[10,11], Sonia Minuzzo[10], Roberta La Starza[12], Giovanni Bernardini[2], Isabella Screpanti[2], Antonio Francesco Campese[2,14] and Maria Pia Felli[1,14]✉

Malignant transformation of T-cell progenitors causes T-cell acute lymphoblastic leukemia (T-ALL), an aggressive childhood lymphoproliferative disorder. Activating mutations of Notch, Notch1 and Notch3, have been detected in T-ALL patients. In this study, we aimed to deeply characterize hyperactive Notch3-related pathways involved in T-cell dynamics within the thymus and bone marrow to propose these processes as an important step in facilitating the progression of T-ALL. We previously generated a transgenic T-ALL mouse model (N3-ICtg) demonstrating that aberrant Notch3 signaling affects early thymocyte maturation programs and leads to bone marrow infiltration by $CD4^+CD8^+$ (DP) T cells that are notably, $Notch3^{high}CXCR4^{high}$. Newly, our in vivo results suggest that an anomalous immature thymocyte subpopulation, such as $CD4^-CD8^-$ (DN) over-expressing CD3ε, but with low CXCR4 expression, dominates N3-ICtg thymus-resident DN subset in T-ALL progression. MicroRNAs might be of significance in T-ALL pathobiology, however, whether required for leukemia maintenance is not fully understood. The selection of specific DN subsets demonstrates the inverse correlation between CXCR4 expression and a panel of Notch3-deregulated miRNAs. Interestingly, we found that within DN thymocyte subset hyperactive Notch3 inhibits CXCR4 expression through the cooperative effects of miR-139-5p and miR-150-5p, thus impinging on thymocyte differentiation with accumulation of $DNCD3\varepsilon^+CXCR4^-$ cells. These data point out that deregulation of Notch3 in T-ALL, besides its role in sustaining dissemination of abnormal DP T cells, as we previously demonstrated, could play a role in selecting specific DN immature T cells within the thymus, thus impeding T cell development, to facilitate T-ALL progression inside the bone marrow.

Oncogene (2024) 43:2535–2547; https://doi.org/10.1038/s41388-024-03079-0

INTRODUCTION

Acute lymphoblastic leukemia (ALL) is a lymphoproliferative disorder caused by the malignant transformation of B- (B-ALL) or T-cell (T-ALL) progenitors. Among childhood acute leukemias, about 60% is ALL, of which 15-20% cases are of T-lineage [1], with a poorer outcome compared with B-ALL [2, 3]. Genetic abnormalities block T-cell precursors differentiation in the thymus and abet abnormal cell proliferation [4]. Accumulating leukemic cells infiltrate the bone marrow (BM) and extramedullary sites [5]. In 60% of T-ALL patients, Notch1 gain-of-function mutation and hyperactivation of Notch3 occurs [6], but Notch3 activating mutations have also been described [7]. Intensive chemotherapy can cure 80% of pediatric patients, but at least 20% of pediatric and 40% of adult T-ALL patients eventually relapse, with poor prognosis. Notch can contribute to chemotherapy resistance [8] therefore, the need to contrast this signaling in T-ALL progression.

Notch is a single-helix transmembrane receptor involved in T-cell development [9] and hemopoiesis and also plays a vital role in the functional regulation of peripheral lymphoid cells, thereby influencing the immune response [10]. In the thymus, the cooperation of Notch with pre-TCR and CXCR4, and then the mature TCR receptor αβ, determine the proliferation, cell fate specification, or death of $CD4^-CD8^-$(DN) BM-derived progenitors [9, 11–13]. Previously, we generated a transgenic mouse model overexpressing the active intracellular-domain of Notch3

[1]Department of Experimental Medicine, Sapienza University of Rome, Rome, Italy. [2]Department of Molecular Medicine, Sapienza University of Rome, Rome, Italy. [3]Department of Translational and Precision Medicine, Sapienza University of Rome, Rome, Italy. [4]Division of Hematology & Medical Oncology, Department of Medicine, Weill Cornell Medicine, New York NY, USA. [5]Center for Life Nano-Neuro Science, IIT, Rome, Italy. [6]A.O.R.N. dei colli Monaldi V., Napoli, Italy. [7]Department of Medical-Surgical Science and Translational Medicine, Sapienza University of Rome, Rome, Italy. [8]Ph.D School of Applied Medical-Surgical Sciences, Department of Biology, University of Rome "Tor Vergata", Rome, Italy. [9]Preclinical Models and New Therapeutic Agents Unit, IRCCS Regina Elena National Cancer Institute, Rome, Italy. [10]Department of Surgery Oncology and Gastroenterology, University of Padua, Padua, Italy. [11]Basic and Translational Oncology Unit, Istituto Oncologico Veneto IOV-IRCCS, Padua, Italy. [12]Hematology Section, Department of Medicine and Surgery, and S. Maria Della Misericordia Hospital Perugia, CREO, Perugia, Italy. [13]These authors contributed equally: Ilaria Sergio, Claudia Varricchio, Sandesh Kumar Patel. [14]These authors jointly supervised this work: Antonio Francesco Campese, Maria Pia Felli. ✉email: mariapia.felli@uniroma1.it

Received: 13 July 2023 Revised: 30 May 2024 Accepted: 5 June 2024
Published online: 21 June 2024

under the proximal *lck* promoter (N3-ICtg) which develops an aggressive disease with a rapid clinical course, sharing multiple aspects with human infantile T-ALL [14]. The persistence of immaturity traits, such as CD25 and the pre-TCR α-chain (pTα) expression, the NF-kB constitutive activation, may alter critical events in DN3/DN4 T cells and lead to deregulated thymocyte growth during the Pre-T/T transition in N3-ICtg mice [14–16]. Progressively, transgenic immature DP T-cells are found in blood circulation, a characteristic common to other Notch models of T-ALL [17]. In particular, we previously demonstrated that pre-leukemic DP T-cells with a high cell-surface expression of CXCR4 and Notch3 ($CD4^+CD8^+Notch3^{+high}CXCR4^{+high}$) prematurely egress from the thymus of N3-ICtg in early leukemia stages and massively infiltrate the N3-ICtg spleen and the BM, a process that can be prevented by CXCR4 antagonism in young (3–4-week-old) N3-IC-Tg mice [18]. We and other groups demonstrated the critical role of CXCR4 and its ligand CXCL12/SDF-1 in Notch-induced T-cell leukemia maintenance and progression and the effect of CXCR4 antagonism in BM infiltration [19, 20].

Notably, during T-ALL progression, the N3-ICtg thymus became precociously fibrous and hypocellular, and here we demonstrate that it is mostly populated by immature $CD3\varepsilon^+$ T-cells with a reduced expression of CXCR4.

Multiple molecular types of machinery regulate CXCR4 expression, by implying transcription factors like E2A and NF-kB [21–23] or epigenetic post-transcriptional regulators of CXCR4 [24–26].

MicroRNAs (miRNAs) play an essential role during both normal and malignant haematopoiesis, including T-ALL [27, 28]. These bioactive small non-coding RNAs, which interact with the complementary sequences in the 3′ untranslated region (3′UTR) of protein-coding mRNA, negatively regulate gene expression by inducing translational repression or mRNA degradation [29]. miRNAs are deregulated in DP cells of N3-ICtg mice [30], and in Notch-1-dependent murine models of T-ALL [31, 32]. However, their role in immature DN thymocytes during development or in T-cell leukemia is poorly known [33, 34]. Presently, in this context, we demonstrate the Notch3-deregulated expression of a panel of miRNAs (miR-150-5p/miR-139-5p/miR9-5p/miR-223-5p) correlated to the altered dynamic of the thymocyte subsets in T-ALL progression. We identify a novel miR-139-5p/miR-150-5p cooperation with Notch, capable to downmodulate CXCR4 gene expression. and to expand $DNCD3\varepsilon^+CD25^+CXCR4^-$ thymocytes which improperly populate the N3-IC-Tg BM.

RESULTS

Notch3-induced expansion of immature DN thymocytes overexpressing CD3ε

Starting from 4 weeks of age, N3-ICtg mice developed an aggressive multicentric T-cell lymphoma with an aberrant pre-T-cell development [14]. At 10-13 weeks, the thymus appeared residual, and the lymphoblastic cells massively infiltrate lymphoid organs in the periphery [17]. In order, to find new molecular mechanisms involved in T-ALL progression, we analyzed the thymocyte subpopulations in 12–14-week-old *wt* and *N3-ICtg* mice, possibly involved in leukemia maintenance. At that age, Notch3 transgenic thymus was hypocellular compared to *wt* mice (Fig. 1A). Flow-cytometric analysis of CD4 and CD8 subsets distribution demonstrated that under the influence of Notch3 overexpression, the percentages (Fig. 1B) and the absolute numbers (Fig. 1C) of DN thymocytes significantly increase in N3-ICtg versus WT mice.

The expression of the CD3ε co-receptor chain on leukemic T cells can be variable but is emerging as a new and valuable target in antileukemic T-cell immunotherapy [35]. CD3ε, is also complexed in pre-TCR and specifically expressed at the thymocyte DN2-DN3 transition phase until the DP stage [36]. Therefore, we analyzed CD3epsilon expression (CD3ε, OKT3), in 12–14-week-old WT and N3-IC-Tg mice. Interestingly, the transgenic DN T-cells were mainly composed of high CD3ε ($DNCD3\varepsilon^+$) expressing cells and displayed a significant increase in the absolute number (Fig. 1D) as well as in the per cell expression of this T-cell marker (Fig. 1E, left panel). Moreover, $CD3\varepsilon^{+high}$ proportion is considerably expanded in the DN subset of N3-ICtg versus WT (Fig. 1E, right panel). Thus, our results, in agreement with sustained pre-TCR expression [16] newly suggested that Notch3 selects a $DNCD3\varepsilon^{+high}$ thymocyte subset by enhancing CD3ε expression, which could represent an effective target of Notch in T-ALL [37].

Progressive maturation of DN thymocytes is dampened by Notch3-induced CXCR4 downmodulation in N3-ICtg mice

Given the cooperative role of pre-TCR, Notch, and CXCR4 in early thymocyte development [11] we evaluated, in the $DNCD3\varepsilon^+$ subset, the expression of CXCR4 cell-surface receptor. In WT mice, no difference is found in the percentage of $DNCD3\varepsilon^+CXCR4^+$ and $DNCD3\varepsilon^+CXCR4^-$ cells (Fig. 2A). The equality of the two subsets agrees with the continued maturation of DN T-cells in a normal thymus. On the contrary, in N3-ICtg thymus, the percentage of $DNCD3\varepsilon^+CXCR4^-$ cells significantly increased (Fig. 2A), in agreement with their higher absolute number in N3-ICtg versus WT thymocytes (Fig. 2B), hence, Notch3 selectively expanded a $DNCD3\varepsilon^+CXCR4^-$ subpopulation.

We also analyzed the expression of CXCR4 in DN3 and DN4 stages, distinguished by staining for CD25 and CD44 by flow cytometry ($CD44^-CD25^+$ and $CD44^-CD25^-$ respectively). Indeed, in 12–14-week-old N3-ICtg mice, DN3 and more evidently DN4 thymocytes displayed a clear decrease of CXCR4 surface expression with respect to WT mice (Supplementary Fig. 1), suggesting a partial differentiative block.

CXCR4 receptor normally anchors preselection thymocytes to the thymic cortex via interaction with its ligand CXCL12/SDF-1*α* on cortical thymic epithelial cells, and disruption of CXCL12/CXCR4 engagements releases preselection thymocytes from the thymic cortex [21]. Indeed, in thymic stromal cells of 6–8-week-old N3-ICtg mice, we previously demonstrated a decreased SDF-1 mRNA expression [38], that could eventually contribute to the egress of immature DP T cells from the thymus. Considering the role of the CXCL12(SDF-1*α*)/CXCR4 system in driving thymocyte progressive maturation across the cortex and medulla [39, 40], we now investigated the ability of DN T cells to migrate. In vitro, SDF-1-induced migration of WT DN thymocytes increased in a dose-dependent manner. Whereas low-CXCR4 expressing DN thymocytes of N3-IC-tg showed a reduced migration ability (Fig. 2C), a potential mechanism to slip away from control in the thymus niche.

Overall, Notch3 modified the thymus microenvironment and could contribute to the aberrant maturation of DN cells with an altered migration capacity, in addition to the decrease of DP T-cells observed in T-ALL progression [38]. $CD5^{Low}$ expression has been associated to leukemic lymphoblasts in T-ALL [41]. Interestingly, $CD5^+$ cells, as well as its expression level (percentages and MFI) inside the $DNCD3\varepsilon^+$ subset is greatly decreased in N3-ICtg (irrespective of CXCR4 surface expression) as compared to *wt* mice (Fig. 2D, left and right panels), suggesting that our model shares this feature with human T-ALL cells [34, 42].

The pro-survival role of CXCR4 and its Notch3-induced down-modulation prompted us to study transgenic thymocyte proliferation and apoptosis. In 12–14-week-old N3-IC-Tg mice, thus at an advanced stage of T-ALL, we assessed by flow-cytometry the expression pattern of Ki67 and Annexin V (Fig. 2E, F). We observed that $DNCD3\varepsilon^+CXCR4^+$ thymocytes proliferate much less in N3-ICtg thymus compared to the CXCR4 negative counterpart (Fig. 2E). Additionally, we evaluated the apoptotic rate, which is associated to a higher expression of Annexin V in the $DNCD3\varepsilon^+CXCR4^+$ thymocytes of the N3-ICtg mice (Fig. 2F).

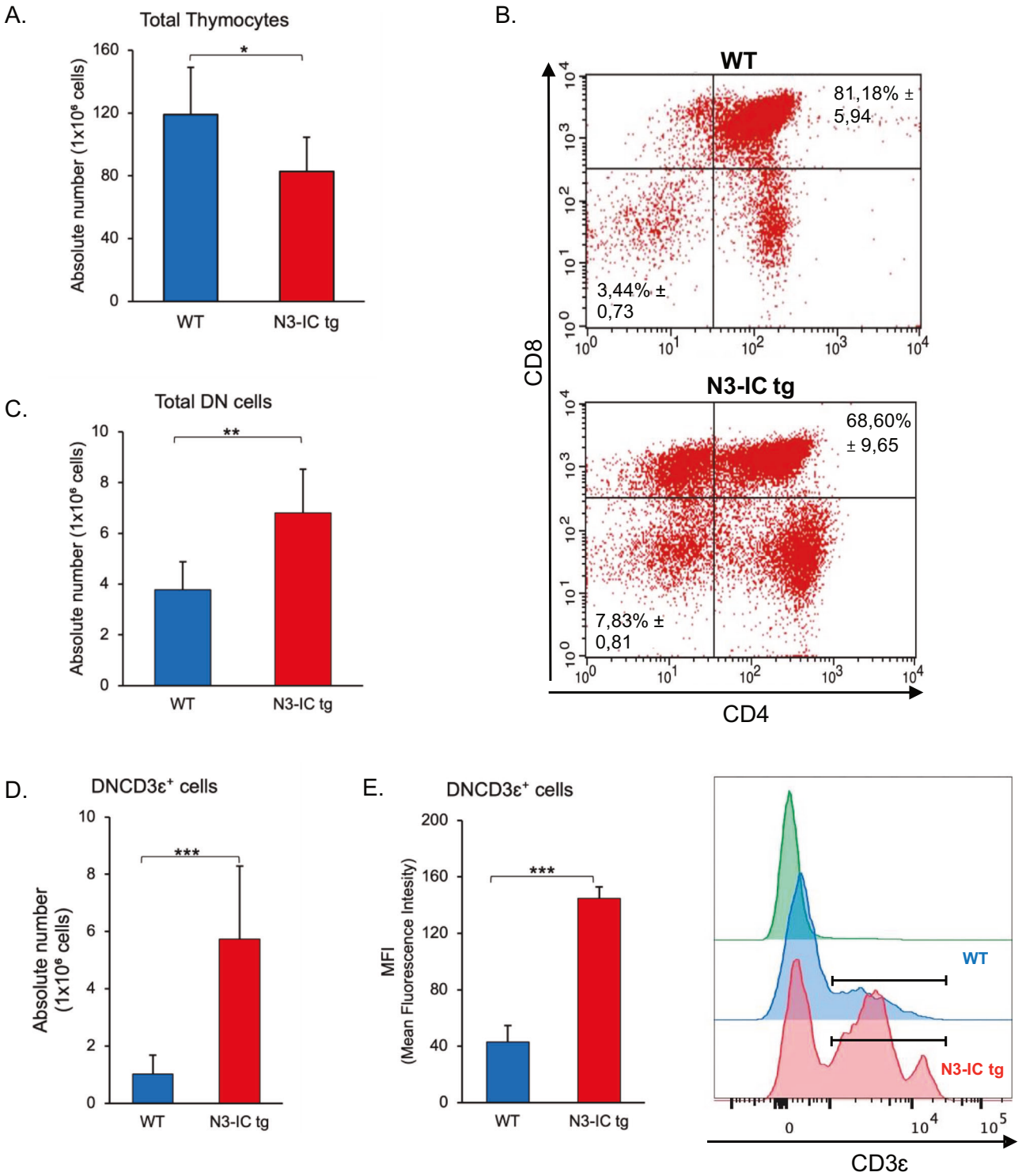

Fig. 1 Notch3 expands the immature CD4$^-$CD8$^-$CD3ε$^{+/high}$ thymocytes. A Absolute numbers of total cell in WT ($n = 6$) and N3-ICtg ($n = 5$) Thymus. **B** Thymocyte subset distribution with average DN and DP percentage ± SD; **C** Absolute numbers of Total DN T-cells in WT ($n = 5$) and N3-ICtg ($n = 4$) mice; **D** Significant higher number of DNCD3ε$^+$ in the N3-ICtg transgenic thymus; **E** Analysis of CD3ε Mean Fluorescence Intensity (MFI) in the DN subset of WT ($n = 7$) and N3-ICtg ($n = 8$) mice. Representative FACS analysis of CD3ε expression; Student's t-test; (*$p < 0.05$; **$p < 0.01$; ***$p < 0.001$).

Therefore, the reduced proportion of DNCD3ε$^+$CXCR4$^+$ subpopulation in the N3-ICtg thymus associates with a decreased proliferative capacity.

The different biological properties of the two N3-IC-tg subsets above may be suggestive of the expansion of the DNCD3ε$^+$CXCR4$^-$ cells unable to progressively mature, depending on reduced migration and responsiveness ability in the thymus microenvironment (see Fig. 2C) as compared to the decrease of DNCD3ε$^+$CXCR4$^+$ cells, anchored to the thymus and possibly still sustaining maturation programs and propagation abilities.

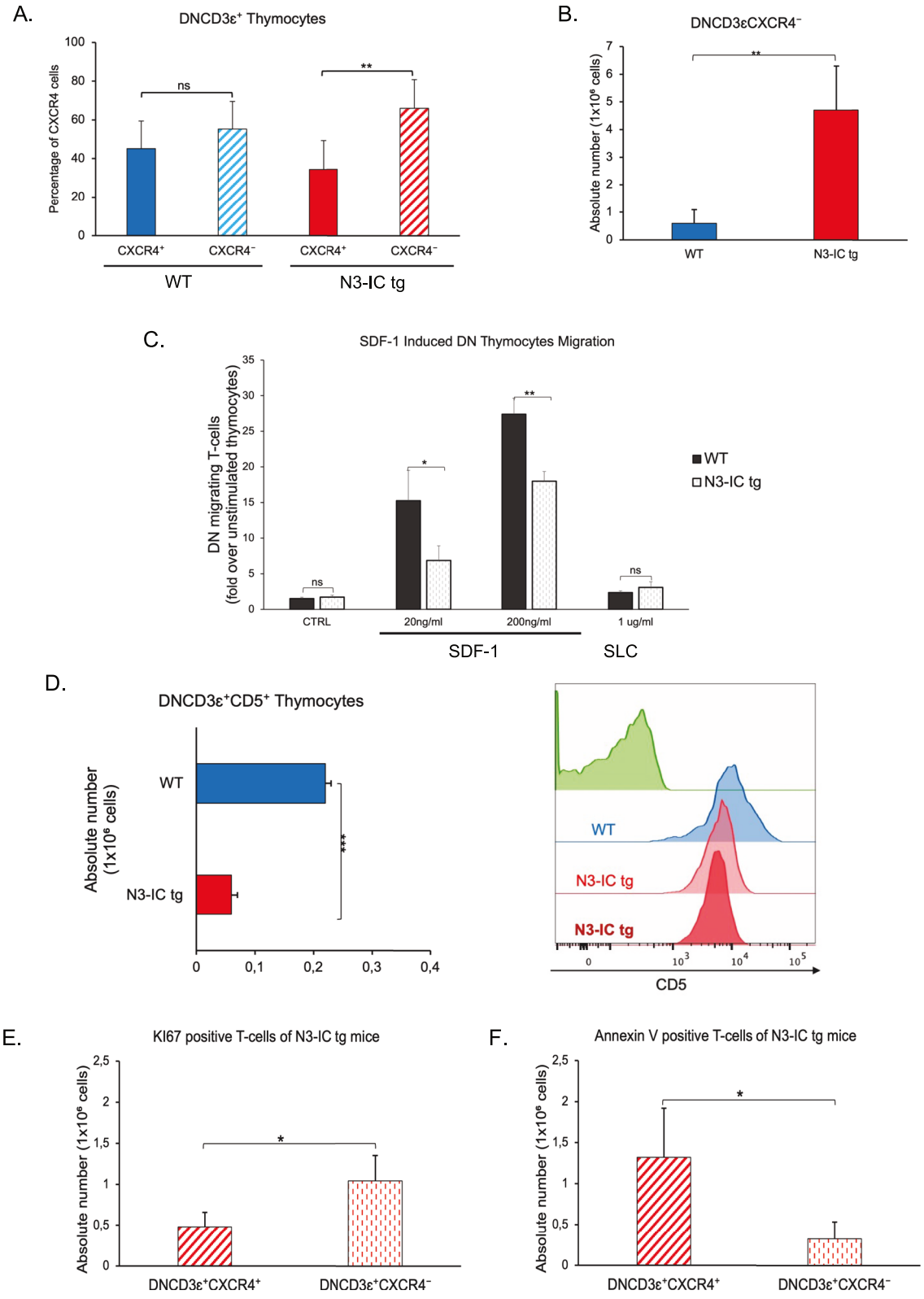

Notch3-modulated microRNAs inversely correlate with cxcr4 gene expression in DN thymocytes

To investigate how Notch3 down-modulates CXCR4, we analyzed the expression of the *cxcr4* gene in purified DN T-cells isolated from the thymus of 12–14-week-old WT and N3-IC-Tg mice.

Starting from the morphological parameters (Supplementary Fig. 2A) the DNCD3ε^{+} sample was further selected by excluding NK1.1, MAC1, and GR1 positive cells in both WT and N3-ICtg mice and any contamination by CD4^{+} and CD8^{+} cells (Supplementary Fig. 2B). RT-qPCR assesses *cxcr4* expression in highly purified DN T-cells. In N3-ICtg mice, *cxcr4* expression was significantly lower than in its WT counterpart (Fig. 3A) Given the positive correlation reported above between CXCR4 and Notch expression, it was intriguing to detect a high expression of the Notch3 gene that it is

Fig. 2 Notch3-induced CXCR4 downmodulation impairs DN T-cells maturation and migration. A Average percentage (±SD) of DNCD3ε$^+$CXCR4$^+$ and DNCD3ε$^+$CXCR4$^-$ thymocyte subsets in WT ($n = 4$) and N3-ICtg ($n = 4$) mice and **B** absolute numbers of DNCD3ε$^+$CXCR4$^-$ of WT ($n = 6$) and N3-ICtg ($n = 8$) mice. **C** Fold increase of DN migrating thymocytes percentages versus unstimulated thymocytes (CTRL), in response to (20 ng/ml and 200 ng/ml) SDF-1 and an unrelated ligand (Secondary Lymphoid Tissue Chemokine, SLC) in WT ($n = 3$) and N3-ICtg ($n = 3$) mice. Each experiment was performed with 12–14-week-old mice. **D** Absolute numbers of DNCD3ε$^+$CD5$^+$ normalized to total DNCD3ε$^+$ thymocytes values in WT ($n = 4$) and N3-ICtg ($n = 4$) mice (12–14-weeks-old), flow-cytometry evaluation of CD5 Mean Fluorescent Intensity (MFI). Evaluation of proliferation and apoptosis of DNCD3ε$^+$CXCR4$^+$ and DNCD3ε$^+$CXCR4$^-$ thymocytes in N3-ICtg mice. **E** Reduced Ki67 levels in the DNCD3ε$^+$CXCR4$^+$ cells of the transgenic concerning DNCD3ε$^+$CXCR4$^-$ cells ($n = 4$); **F** Higher expression of Annexin-V in the DNCD3ε$^+$CXCR4$^+$ thymocytes of N3-ICtg mouse concerning DNCD3ε$^+$CXCR4$^-$ ($n = 4$). Results represent mean ± SD. (*$p < 0.05$; **$p < 0.01$; ***$p < 0.001$; ns=not-significant); Student's *t*-test.

still found in these selected transgenic DN thymocytes (Fig. 3B), at this stage of the disease. The data also support the inverse correlation between β-arrestin (Fig. 3C) and CXCR4 expression, as we previously demonstrated by in silico analysis of a selected T-ALL patient subgroup [39].

To investigate how Notch3 downregulates CXCR4 inside DNCD3ε$^+$ subset, we considered the emerging role of microRNAs (miRNAs) as clinical diagnostics and therapeutic targets in human diseases. Recently, interesting studies highlighted miRNAs involvement also in T-ALL [43]. In addition, microarray analysis demonstrated the modulation of miRNA profile in DP thymocytes in our Notch3-dependent T-ALL model, such as miR-223, regulated by Notch/NF-κB partnership, and miR-139-5p [30]. Both miRNAs share a putative Notch effector consensus site, RBPjK, evolutionarily conserved between human and mouse. The 3′UTR of the *cxcr4* gene was studied using bioinformatic tools for the prediction of putative miRNA binding sites, namely miRbase and TargetScan (Fig. 3D). The analysis identified three miRNAs conserved between human and mouse: miR-150-5p, miR-139-5p, and miR-9-5p that target *cxcr4* 3′UTR in different tumors [44–46]. The miR-139-5p and miR-9-5p and the *cxcr4* 3′UTR itself are evolutionarily conserved, between humans and mice, in their sequence at the binding site. Newly, miR-139-5p appears to bind two contiguous sites to the 3′UTR of *cxcr4* in mice. The first site has the sequence at position 267–274, conserved in most vertebrates, including humans and mice (site: TargetScanHuman 7.2, [47]).

Notably, in 12–14-week-old mice, the expression of miR-150-5p, miR-139-5p and miR-9-5p, monitored by digital droplet PCR (ddPCR), in selected DNCD3ε$^+$ thymocytes significantly increased in transgenic mice when compared with WT (Fig. 3E). Although, miR-9-5p is poorly represented (0.09copies/μl ± 0.02) nor increased suggesting a minor role in this context. Few reports demonstrated that miR-150-5p targets the 3′UTR of *cxcr4* only in non-neoplastic contexts [48, 49]; notably, the miRNA-binding site of the 3′UTR of *cxcr4* is conserved between human and mouse; whereas, the binding sequence of *cxcr4* differs by a few nucleotide bases (site:TargetScanHuman 7.2, [47]). Interestingly, the marked increase of miR-150-5p at the DN stage (Fig. 3E) was in opposition to the great decrease described at the DP stage in N3-IC-tg mice [30] and to the downmodulation observed in the normal hematopoietic process [50], thus evidencing a critical role of this miRNA along T-cell development and leukemia [51]. MiR-150-5p and miR-139-5p high expression (Supplementary Fig. 3A-B) and miR-223 low expression was observed in the same samples of transgenic DNCD3ε$^+$ T-cells (Supplementary Fig. 3C); in contrast to its reported high expression in transgenic DP [30]. Therefore, Notch3 differently modulated this miRNA in distinct T-cell maturation stages.

Based on previous results, we analyzed ex-vivo DNCD3ε$^+$ T cells derived from N3-ICtg thymus and purified as described above. We first selected DNCD3ε$^+$ cells and then distinguished for positive or negative CXCR4 expressing cells (Fig. 3F) (for check purity, see Supplementary Fig. 4).

The predominant DNCD3ε$^+$CXCR4$^-$ cells had fivefold lower mRNA levels of *cxcr4* than the smaller DNCD3ε$^+$CXCR4$^+$ (Fig. 3G) subpopulation. This evidence suggested a direct correlation between mRNA level and cell-surface expression of CXCR4 in selected DN T-cells. Additionally, both miR-150-5p and miR-139-5p expression levels are inversely correlated to CXCR4 mRNA level (Fig. 3G).

Therefore, our ex-vivo experiments supported the hypothesis of a post-transcriptional role of Notch3 in regulating CXCR4 expression and for the first time suggest CXCR4 as a new potential target of miR-150-5p and miR-139-5p in Notch-induced T-ALL.

miR-139-5p and mir-150-5p cooperate in downmodulating CXCR4 expression in transgenic N3-232T-cell line

To confirm data above in an in vitro system, murine N3-232T cell line, established from a 6-week-old N3-IC-Tg thymus [14] was transfected with miR-139-5p mimic (100 nM) and its negative control miRNA (CTRL-;100 nM) using the Neon transfection system (Fig. 4A). After 72 h, we assessed the expression of the endogenous CXCR4 receptor by flow-cytometry. The CXCR4-membrane down-modulation is shown by the overlay of miR-139-5p mimic transfected (MFI 910.00 ± 140.0) versus control (CTRL-) cells (MFI 1096.66 ± 144.0) (Fig. 4A, right-panel). In parallel, RT-qPCR demonstrated the reduced *cxcr4* gene transcript in miR-139-5p transfected as compared to CTRL- cells (Fig. 4A, left-panel), and transfection efficiency (Supplementary Fig. 5A). To demonstrate a specific correlation between miR-139-5p and CXCR4, we transfected N3-232-T cells with antagomiR-139-5p at 100 nM (Fig. 4B) and monitored transfection efficiency (Supplementary Fig. 5B). Our results, 72 h post transfection, in antagomir-transfected-, as compared to the CTRL- cells, showed a significant increase in CXCR4 mRNA expression (Fig. 4B, left panel), as well as in CXCR4 cell-surface expression, as measured by MFI value (Fig. 4B, right panel, 850.00 ± 36.5 vs 709.54 ± 15.1, respectively).

Moreover, we analyzed miR-150-5p effects on endogenous CXCR4 expression through RT-qPCR and flow-cytometry analysis, 72 h post-transfection of N3-232-T cells with miR-150-5p mimic 100 nM (Fig. 4C). We demonstrated that mimic decreased CXCR4 mRNA level (Fig. 4C, left panel), correlating with the flow-cytometry data (Fig. 4C, right panel), showing increased percentages of transfected N3-232-T cells (30,30% ± 1.8) with reduced cell-surface receptor expression as compared to CTRL-. The Transfection efficiency was verified (Supplementary Fig. 5C). Consequently, we demonstrated an inverse correlation between miR-150-5p expression levels and CXCR4 mRNA and protein expression. The specific effect of miR-150-5p was also assayed by its Antagomir and results shown in Fig. 4D demonstrated the increased expression of CXCR4 expression at both mRNA and cell-surface protein levels.

The convergent inverse correlation between miR-139-5p and miR-150-5p with CXCR4 expression and their simultaneous high expression in a specific T-cell context, DNCD3ε$^+$CXCR4$^-$ cells, prompted us to carry out further experiments to explore the possible combined effect of both miRNAs. After 72 h, the N3-232-T cells co-transfected with both miR-139-5p and miR-150-5p mimics show a more significant reduction of CXCR4 surface expression with respect to CTRL- (Fig. 4E, right panel). Accordingly, the left panel of Fig. 4E shows the inverse correlation between

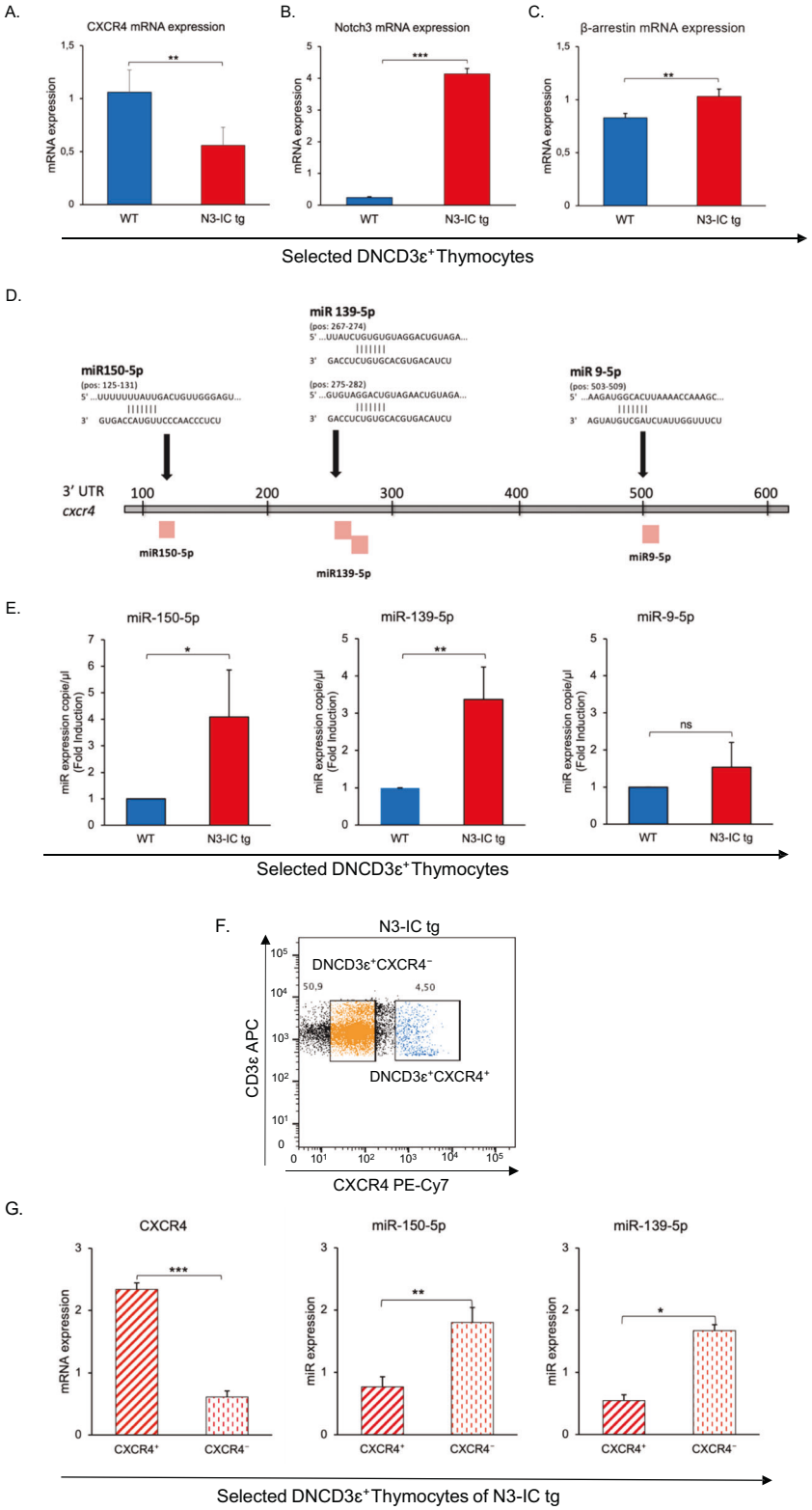

Fig. 3 CXCR4 expression inversely correlates with miR139-5p and miR150-5p in transgenic DNCD3ε^{+} thymocytes. Selection of DN thymocytes negative for NK1.1, MAC1 and GR1- in WT ($n = 5$). The same strategy was used for N3-ICtg mice ($n = 6$); in these selected thymocytes, **A** CXCR4 mRNA levels are drastically reduced, in contrast to **B** Notch3 gene expression still high in N3-ICtg mice, and **C** the increased β-arrestin1 mRNA levels in N3-ICtg ($n = 4$) comparing WT ($n = 4$) mice. **D** Putative sites of miR-150-5p, miR-139-5p and miR-9-5p on the 3′UTR target of the cxcr4 gene (TargetScan and miRbase software). **E** Digital-droplet-PCR (ddPCR) of miR-150-5p, miR-139-5p, and miR-9-5p in selected DNCD3ε^{+} thymocytes of 12–14-week-old WT ($n = 4$) and N3-ICtg ($n = 4$) mice; **F** Positive selection for DNCD3ε^{+} followed by positive and negative selection for CXCR4 by sorting analysis; **G** Evaluation of CXCR4 transcript expression, and miR-150-5p and miR-139-5p in the DNCD3ε^{+}CXCR4^{+} and DNCD3ε^{+}CXCR4^{-} subpopulations. Student's *t*-test (*$p < 0.05$; **$p < 0.01$; ***$p < 0.001$; ns not significant).

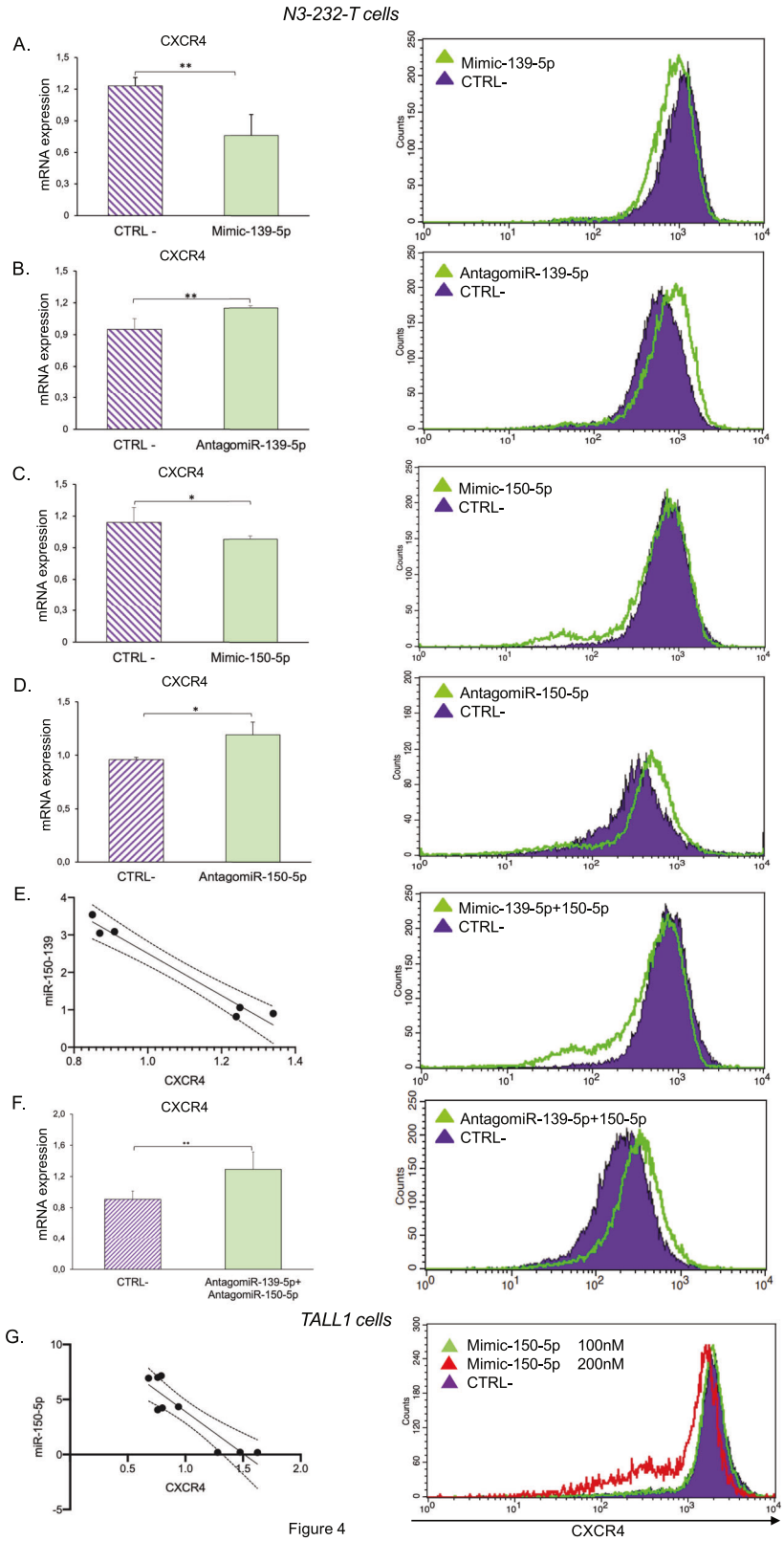

Figure 4

overexpression of miR-139-5p/miR150-5p (Supplementary Fig. 5D) and CXCR4 mRNA expression, further sustained by RT-qPCR analysis of CXCR4 mRNA levels (Supplementary Fig. 5E), as compared to the negative control (CTRL-) and cells transfected with the single mimic, respectively mimic-139-5p and mimic-150-5p (Fig. 4A and C). Dissection of the regulation by miRNAs involved the analysis of the combined Antagomirs effect. N3-232T cells were transfected with the Antagomir150-5p and 139-5p combo which greatly increased CXCR4-membrane expression (Fig. 4F, right panel) as shown also by the down-modulation of CXCR4 mRNA expression (Fig. 4F, left panel). In summary, for the first time, our data demonstrated an inverse correlation between

Fig. 4 The cooperative function of miR-150-5p and miR-139-5p reduces CXCR4 expression in murine and human T-ALL cell lines. Analysis of CXCR4 mRNA levels (left-panels) and cell-surface expression (right-panels) in N3-232-T and TALL1 cells 72 h post transfection with the negative control (CTRL−), and with single or combined miRNAs. **A** Mimic miR-139-5p at 100 nM, CXCR4 mRNA and membrane expression; **B** antagomiR-139-5p at 100 nM, CXCR4 mRNA and cell-surface expression; **C** mimic miR-150-5p at 100 nM, CXCR4 mRNA and membrane expression; **D** antagomiR-150-5p at 100 nM, CXCR4 mRNA and cell-surface expression, **E** correlation analysis between CXCR4 mRNA, miR-139-5p and miR-150-5p expression levels and decreased CXCR4 surface expression; **F** correlation between CXCR4 mRNA, antagomir-139-5p and antagomiR-150-5p expression levels, and increased CXCR4 cell-surface expression. **G** Human TALL1 cells transfected with increasing miR-150-5p (100 and 200 nM), correlation analysis between CXCR4 mRNA and miRNAs levels. mRNA levels are expressed as the average value ± SD. Student's *t*-test (*$p < 0.05$; **$p < 0.01$). Pearson-r test (***$p < 0.001$ Fig. 7E, F).

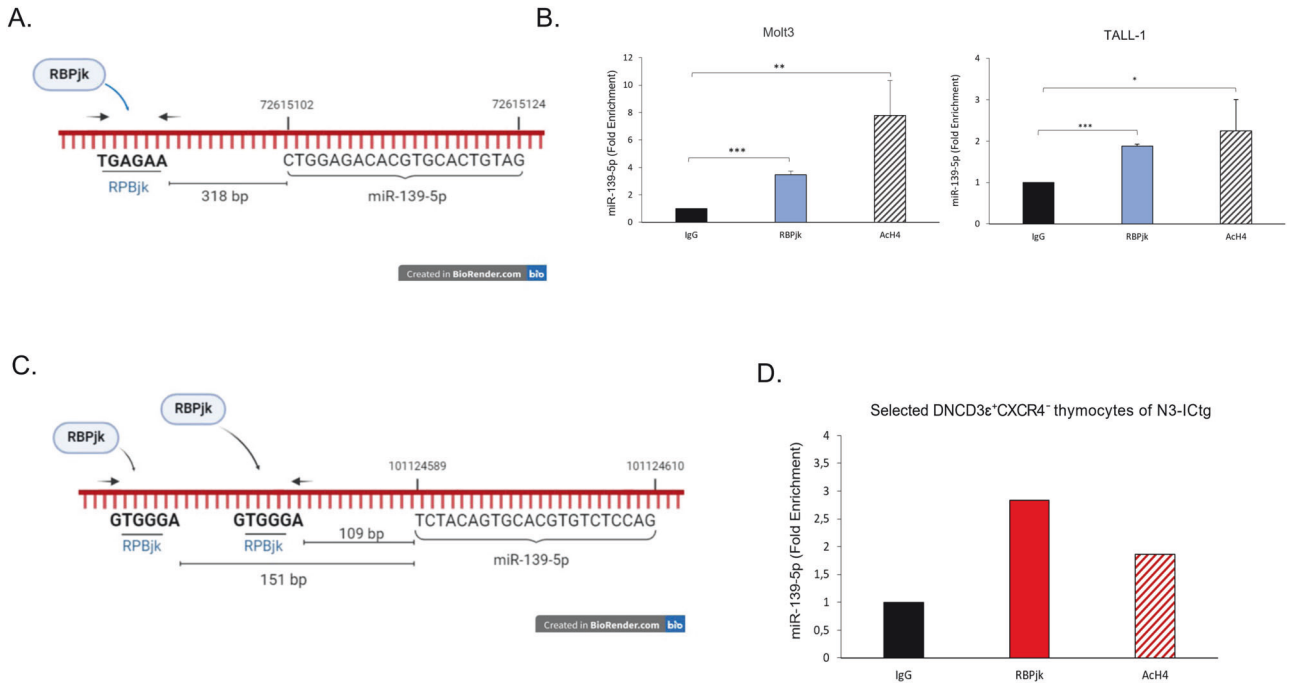

Fig. 5 Analysis of RBPjk occupancy in human and murine miR-139-5p promoter. A graphical representation of human miR-139-5p promoter region. RBPjk binding site is shown. **B** Crosslinked protein-DNA complexes from Molt3 and TALL1 cell lines were subjected to immunoprecipitation with antibodies against RBPjk and AcH4. The immunoprecipitated DNA samples were amplified by RT-qPCR using miR-139-5p promoter-specific primers which encompass one RBPjk binding site (as indicated in **A**). **C** Graphical representation of murine miR-139-5p promoter region. Two RBPjk binding sites are shown. **D** Purified DNCD3ε^{+}CXCR4 negative thymocytes from a pool of N3-ICtg mice ($n = 10$) were crosslinked and immunoprecipitated with anti-RBPjk and anti-AcH4 as described above in B). Amplification of the immunoprecipitated DNA samples was performed by RT-qPCR with promoter-specific primers primers which encompass both RBPjk binding sites as shown in **C**, for murine miR-139-5p. Results are shown as the mean average ± SEM of three (Molt3) and two (TALL1) independent experiments. Student's *t*-test (*$p < 0.05$; **$p < 0.01$, ***$p < 0.001$).

miR139-5p/150-5p and CXCR4 expression and the cooperative effect of these two miRNAs in the T-ALL context.

Overexpressed miR-150-5p functionally cooperates with endogenous miR-139-5p to downmodulate CXCR4 in human TALL-1 cells

To support our data above, we extended the in vitro studies in a human T-ALL cell line, TALL-1, overexpressing Notch3 and previously demonstrated to be highly positive for CXCR4. In that cell context, Notch3 silencing downmodulated CXCR4 cell-surface expression through a β-Arrestin1-dependent mechanism [38]. TALL1 cells, with an immature DP phenotype, endogenously express miR-139-5p at a high level, as already demonstrated [30, 45]; conversely, miR-150-5p is nearly undetected (Supplementary Fig. 6A, CTRL), in agreement with previous reports [30, 51].

Based on this evidence, and to prove the combined action of the two miRNAs, we transfected increasing amounts of mimic miR-150-5p, 100 and 200 nM (Supplementary Fig. 6A), and the relative negative control (CTRL-). Seventy-two hours post-transfection, the highest level of miR-150-5p (200 nM) increases the percentage of TALL1 cells with reduced CXCR4 membrane expression (Fig. 4G, right panel) further supported by the inverse correlation of the miRNAs with CXCR4 mRNA levels (Fig. 4G, left panel) and by RT-qPCR analysis displaying the decreased CXCR4 mRNA level already at 100 nM of miR-150-5p (Supplementary Fig. 6B).

RBPjk site occupancy is common to active miR-139-5p promoter in human and murine T-ALL

To deepen our study on miRNA regulation in a Notch-induced T-ALL context and considering the relationship between Notch and miR-150 and miR-223 transcriptional regulation [30, 51], we inspected the human promoter of miR-139-5p and identified an RBPjk binding site. This transcription factor is the main transcriptional effector of Notch signaling [9]. As shown in Fig. 5A, the RBPjk consensus site (5′-TGATAA-3′) is localized 324 bp upstream of the human miR-139-5p sequence. To analyzed if RBPjk was able to bind human miR-139-5p promoter, we conducted a Chromatin immunoprecipitation assay in Molt3 (Notch1-dependent) and TALL-1 (Notch3-dependent) T-ALL cells. Surprisingly, we observed that the miR-139-5p promoter is transcriptionally active in Molt3

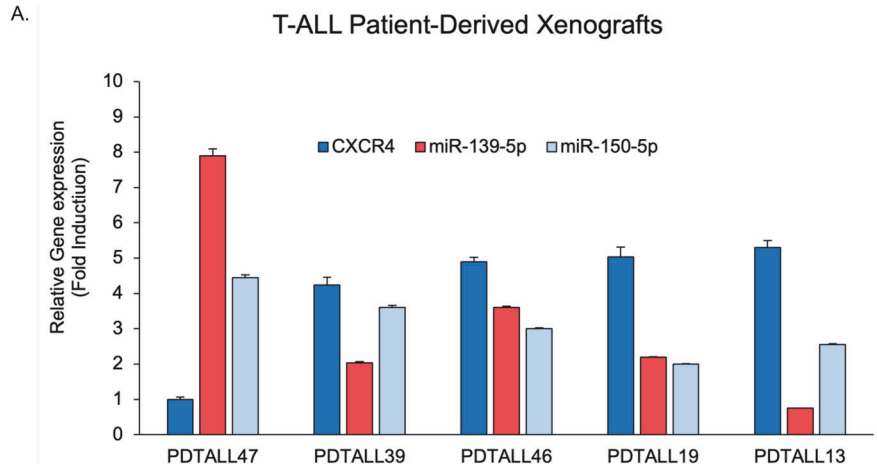

Fig. 6 CXCR4 expression is inversely correlated to miR-150 and miR-139 in patient-derived xenograft (PDTALL). For each of the five samples of PDTALL were analyzed by RT-qPCR CXCR4 mRNA and miR-139-5p and miR-150-5p expression. The results shown in the figure are expressed as the mean average deviation of two separate experiments.

and TALL1 cells, as documented from the hyperacetylated chromatin status (AcH4 bars in the graph of Fig. 5B), and that RBPjk is efficiently recruited in both cell lines (compare IgG with RBPjk bars in graphs of Fig. 5B). Interestingly, analysis of murine miR-139-5p promoter sequence has revealed the presence of two RBPjk binding sites (5′-GTGGGA-3′) located at 157 bp and 115 bp upstream of the miRNA sequence, respectively (Fig. 5C). The ChIP assay was performed using purified DNCD3ε$^+$CXCR4$^-$ thymocytes obtained from a pool of ten Notch3-ICtg mice and by immunoprecipitation of RBPjk and the acetylated histone H4 to confirm the promoter activation status. Results clearly indicated that RBPjk strongly bound the transcriptionally active miR-139-5p promoter (Fig. 5D) also in the murine context. These data strengthen the role of the Notch effector RBPjk in miRNA-mediated CXCR4 regulation and, for the first time, demonstrate a mechanism of direct control of Notch on miR-139-5p transcriptional regulation that is common to both human and murine T-ALL.

CXCR4 expression is inversely correlated with miR-150-5p and miR-139-5p expression in T-ALL patient-derived samples

To extend our results to human T-ALL patients, we analyzed the expression of CXCR4, as well as miR-150-5p and miR-139-5p in a panel of patient-derived xenograft models established from clinical samples in NOD/SCID mice [52, 53]. As shown in Fig. 6, we analyzed five xenografts characterized by Notch1 mutation except for PDTALL13, with no Notch1 mutation. In all the samples we detected the inverse correlation between CXCR4 expression and miR-150-5p and miR-139-5p expression, as evaluated by RT-qPCR. Interestingly, the Notch1 mutated PDTALL47 and the Notch1-unmutated PDTALL13 display really the opposite for what concern CXCR4 and the two miRNAs expression. Our results strengthen the possible role of Notch-induced miRNA-mediated CXCR4 regulation, also in PDX with human T-ALL patient cells.

Lack of membrane CXCR4 enhances vasculature-associated circulating DNCD3ε$^+$ T cells in N3-ICtg mice

CXCR4 regulates leukemia homing/infiltration into lymphoid organs and promotes T-ALL cell invasion [54]. Moreover, CXCR4 is responsible for anchoring and retaining thymic-resident T-cells within the cortex for progressive maturation [21].

On these premises and based on the results so far obtained about the expanded DNCD3ε$^+$CXCR4$^-$ T-cells in (12–14-week-old) transgenic mice, we investigated whether CXCR4 down-modulation could influence the dissemination of this subset as T-ALL progresses. To sustain our hypothesis, we did a tail injection of CD45.2-PE antibody: CD45.2$^+$ cells are referred to as vasculature-associated circulating while CD45.2 negative (CD45.2$^-$) are considered parenchymal and so residing in the tissue [55, 56]. NK1.1$^+$ cells, that express CXCR4, were excluded from the analysis (Supplementary Fig. 7). In N3-IC-Tg thymus, we observed a higher percentage of DNCD3ε$^+$CD25$^+$CD45.2$^+$ gated cells (Fig. 7A, left panel), possibly representing high motile cells, localized in the perivascular zone, with respect to wt counterpart. Intriguingly, CXCR4 negative cells dominated this transgenic DNCD3ε$^+$CD25$^+$CD45.2$^+$ subpopulation, with a tenfold increase compared to CXCR4$^+$ cells (Fig. 7A, right panel). These results agreed with increased DNCD3ε$^+$CD45.2$^+$ cells most prominently CXCR4 negative (Supplementary Fig. 8B) and suggested that thymocytes lacking CXCR4 membrane expression, in the DNCD3ε$^+$ subset, could be more prone to circulation. Indeed, DNCD3ε$^+$CD25$^+$ cells greatly increase in transgenic BM concerning WT (Fig. 7B, left panel) and display a higher percentage of CXCR4 negative T Cells (Fig. 7B, right panel). Of Note, DNCD3ε$^+$CD25$^+$ subpopulation is almost absent in WT BM.

Collectively our results suggest that Notch3-induced CXCR4 downmodulation could favor the egress of thymocytes and result in a deep thymus depletion in advanced T-ALL progression (Fig. 1A).

Additionally, the gated DNCD3ε$^+$CD25$^+$CD45.2$^+$ cells (Supplementary Fig. 9C) are quite equally and low represented in the of BM of WT and N3-ICtg in which, however, prevail the CXCR4$^+$ cells.

DISCUSSION

In this study, we investigated the Notch3-modulated pathway/s that altered thymocyte dynamics and lead to the anomalous BM infiltration by immature DN T-cells, in advanced stages of T-ALL.

Impaired DN thymocyte development in N3-IC-tg mice enhanced the generation of DN3 (CD44$^-$CD25$^+$) thymocytes with low/absent CXCR4 expression also common to the reduced DN4 (CD44$^-$CD25$^-$) subset, thus suggesting a stage-specific Notch3 effect on CXCR4. Namely, Transgenic DNCD3ε$^+$CXCR4$^-$ T-cells accumulate inside the thymus, became less responsive to CXCL12-SDF1 stimulus, which decreased their ability to migrate, and potentially to respond to thymic microenvironment signals for maturation and retention. Therefore, expanded DNCXCR4$^-$ cells are unable to progressively mature, slip away from control, and are possibly free to egress from the thymus and disseminate. Conversely, Notch3-restricted DNCD3ε$^+$CD5$^-$CXCR4$^+$ cells could represent the small subset of quiescent thymocytes that persisted normally anchored to the thymus, potentially for disease relapse,

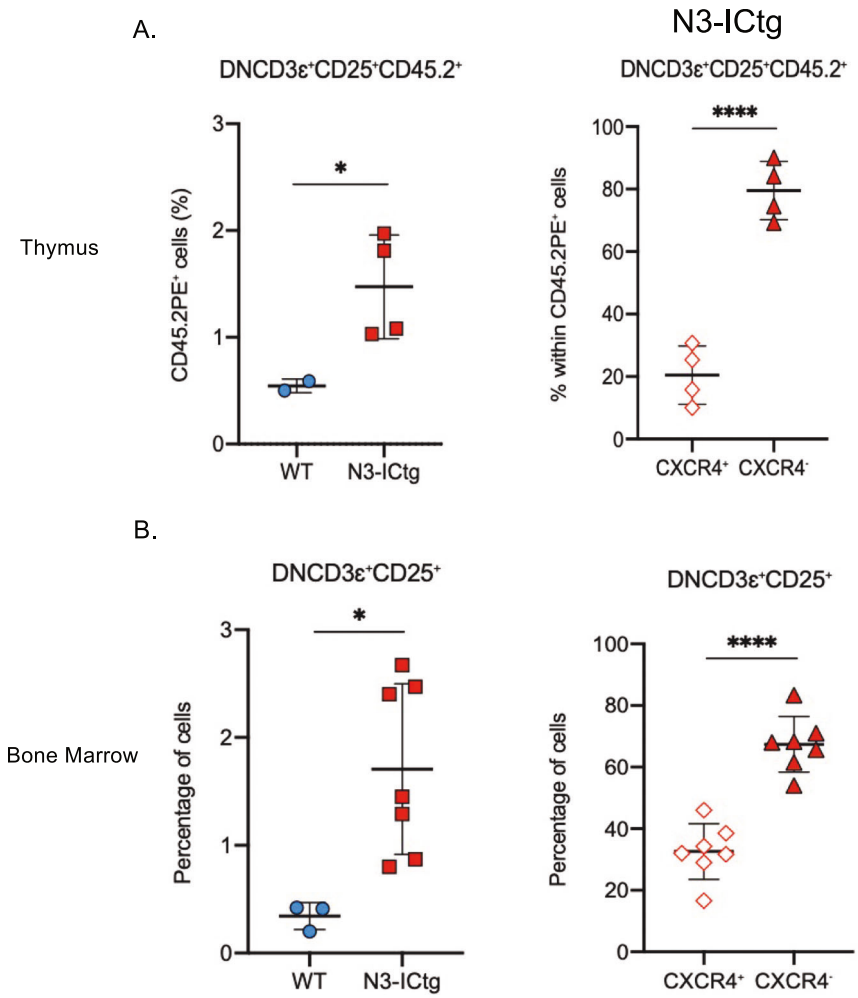

Fig. 7 In vivo CD45 labeling reveals the high level of vasculature-associated DNCD3ε$^+$CD25$^+$ in N3-ICtg thymus possibly invading transgenic bone marrow. In vivo CD45 labeling of T cells in 12–14-week-old WT ($n = 2$) and N3-ICtg mice ($n = 4$); **A** The percentage of DNCD3ε$^+$CD25$^+$CD45.2$^+$ in the thymus of N3-ICtg as compared to WT, and the frequency of transgenic CXCR4$^+$ and CXCR4$^-$ cells (right-panel). **B**) The percentage of DNCD3ε$^+$CD25$^+$ T cells in the BM of N3-ICtg ($n = 7$) concerning WT mice ($n = 3$), and the frequency of transgenic CXCR4$^+$ and CXCR4$^-$ cells (right panel). Student's *t*-test (*$p < 0.05$; ****$p < 0.0001$).

but with a reduced self-renewal capacity (Fig. 2E, F) and capability to generate mature and immunocompetent cells. We theorize that this defective Notch3 transgenic thymus might disrupt the natural cell competition between 'old'-thymus- and 'young'-BM-resident leukemic cells known as a tumor suppressor mechanism within the thymus [57, 58].

To unbalance the thymus-resident thymocyte subsets, Notch3 operated through a miRNA-based mechanism which negatively regulated CXCR4 expression and expanded the immature DNCD3ε$^+$CD5$^-$CXCR4$^-$ subset. We analyzed in DN T cells a panel of four miRNAs: miR-9-5p, miR-139-5p, miR-150-5p expression, comparatively to miR-223. Indeed, while we have a quite detailed knowledge of different transcription factors in DN stages [59], underexplored is the role of miRNAs in DN thymocyte [34], and to be studied in T-ALL development. In Supplementary Fig. 3C, we evidenced a high expression of miR-223-5p in selected WT DN T-cells compared to low miR-150-5p and miR139-5p levels. Newly, we demonstrated the cooperative function miR-139-5p/miR-150-5p that by downregulating CXCR4 had a double effect on N3-IC-Tg thymus: to interfere with T-cell progressive maturation and to enhance the presence of an immature DNCD3ε$^+$CD5$^-$CXCR4$^-$ T-cells close to the perivascular zone prone to egress and to anomalously infiltrate the BM. We would favor the hypothesis that these immature T-cell subset may sustain T-ALL progression, once migrated in the BM.

We demonstrated that the cooperation of the two miRNAs is a common mechanism in murine and human T-ALL cells. Interestingly, standing the high expression of miR-139-5p in the human TALL1 [30], increasing concentrations of miR-150-5p (100–200 nM) are required to downmodulate the expression of the endogenous CXCR4 receptor. Interestingly, we individuated one binding motifs for RBPjk in the human and two in the murine miR-139-5p promoter. Newly, our data demonstrated in vivo the occupancy of RBPjk site in the transcriptionally active promoter of human and murine T-ALL cells.

Identifying microRNAs involved in pediatric T-ALL with the potential to become critical diagnostic tools for classification and monitoring clinical outcomes is an unmet need in hematological malignancies. Few papers analyzed microRNA profiles in T-ALL [28], mostly to distinguish B- to T-ALL [60, 61] or in adult leukemia [62, 63]. Interestingly, our data individuated a panel of four miRNAs that we would suggest for the miRNA signature still not available for T-ALL. Of note, no paper reported about the deregulated expression of miRNAs in DN T-cells, a subset to be deeply studied since strictly related to leukemia development as demonstrated in Lmo2-induced T-ALL [58, 64].

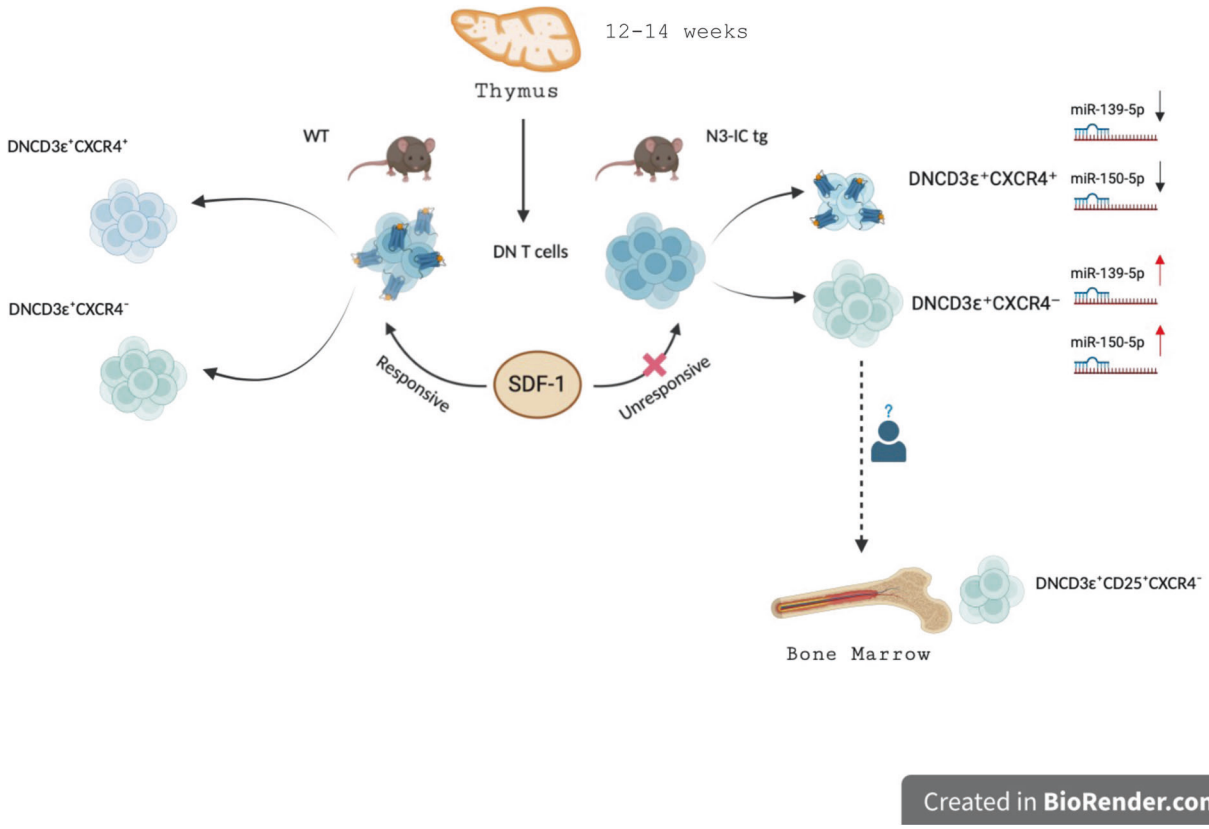

Fig. 8 Graphical representation of the dynamic changes subverting the transgenic N3-ICtg thymus at 12–14 weeks of age. Our model suggests the interesting new Notch/miRNAs crosstalk impinging on the differentiation and dissemination programs dominating advanced stages of the T-ALL and highlights the important role of the thymus that is poorly understood.

Notably, For the first time, we observed an inverse correlation between the expression of CXCR4 and two miRNAs, miR-150-5p and miR-139-5p also in patient-derived xenograft, thus sustaining the importance of miRNAs/CXCR4 crosstalk in human Notch induced T-cell leukemia.

In conclusion, as depicted in Fig. 8 our studies demonstrated how dynamic are changes in the thymus microenvironment and the central role of this lymphoid compartment [65] not only in early [39, 66], but also in later events of T-ALL progression. The progressive depletion of thymus operated by Notch3 may suggest two possible scenarios: thymus microenvironment could represent the reservoir of a leukemia-initiating cells and/or the future niche for immature leukemic T cells coming from the BM. Future studies are required to detail how (re)circulation of T lymphoblasts between these two different lymphoid organs occurs, but our studies strongly underline the strategic role of the thymus in T-ALL progression.

MATERIAL AND METHODS

Mice

N3-ICtg mice [67] were bred and maintained as reported in [68] and detailed in Supplementary Information.

Cell culture

Murine N3-232T cells maintained as described elsewhere [14]. Human TALL1 and Molt3 cells were maintained as described in [7]. Details are in Supplementary Information.

Flow cytometry

T-cells from the thymus and BM were processed as described in [15] and antibodies are described in Supplementary Information.

Isolation of DN T-cell subsets by fluorescent-activated cell sorting. Thymocytes of 12–14-week-old N3-ICtg mice were stained and selected according to the protocols in Supplementary Information.

Migration assay

In vitro CXCL12/SDF-1-induced migration was performed with thymocytes as previously described [39]. See details in Supplementary Information.

Transfections of N3-232T and TALL-1 cell lines

N3-232T cells were transfected with miR-139-5p, AntagomiR-139-5p, and miR-150-5p, while TALL1 with increasing levels of miR-150-5p by using Neon Transfection System (Invitrogen). All details are described in Supplementary Information.

RNA extraction and RT-qPCR and Droplet digital PCR (ddPCR)

Total RNA extraction, reverse-transcription and RT-qPCR are reported in Supplementary Information. Droplet digital PCR (ddPCR) was performed using the Bio-Rad QX200 System (Bio-Rad Laboratories, Hercules, CA, USA) following the manufacturer's protocol. See details in Supplementary Information.

Chromatin immunoprecipitation assay (ChIP assay) of human and murine T-ALL cells

Human T-ALL cell lines, TALL-1 and Molt3, and purified DNCD3ε^+CXCR4 negative thymocytes from N3-ICtg mice ($n = 10$) were used for ChIP experiments described in Supplementary Information.

In vivo intravenous CD45 labeling and analysis of thymic DN T-cells

In vivo labeling and analysis of DN CD3ε^+ thymocytes in the thymic perivascular spaces, see detailed information in Supplementary Information.

Statistical analysis

Analysis of results performed according to the protocols in Supplementary Information.

DATA AVAILABILITY

The raw data supporting the conclusions of this article will be made available by the authors, without undue reservation, to any qualified researcher.

REFERENCES

1. Chiaretti S, Li X, Gentleman R, Vitale A, Vignetti M, Mandelli F, et al. Gene expression profile of adult T-cell acute lymphocytic leukemia identifies distinct subsets of patients with different response to therapy and survival. Blood. 2004;103:2771–8.
2. Matthijssens F, Sharma ND, Nysus M, Nickl CK, Kang H, Perez DR, et al. RUNX2 regulates leukemic cell metabolism and chemotaxis in high-risk T cell acute lymphoblastic leukemia. J Clin Investig. 2021;131:e141566.
3. McMahon CM, Luger SM. Relapsed T cell ALL: current approaches and new directions. Curr Hematol Malig Rep. 2019;14:83–93.
4. Scupoli MT, Donadelli M, Cioffi F, Rossi M, Perbellini O, Malpeli G, et al. Bone marrow stromal cells and the upregulation of interleukin-8 production in human T-cell acute lymphoblastic leukemia through the CXCL12/CXCR4 axis and the NF-kappaB and JNK/AP-1 pathways. Haematologica. 2008;93:524–32.
5. Chiaretti S, Zini G, Bassan R. Diagnosis and subclassification of acute lymphoblastic leukemia. Mediterr J Hematol Infect Dis. 2014;6:e2014073.
6. Chiang MY, Radojcic V, Maillard I. Oncogenic Notch signaling in T-cell and B-cell lymphoproliferative disorders. Curr Opin Hematol. 2016;23:362–70.
7. Bernasconi-Elias P, Hu T, Jenkins D, Firestone B, Gans S, Kurth E, et al. Characterization of activating mutations of NOTCH3 in T-cell acute lymphoblastic leukemia and anti-leukemic activity of NOTCH3 inhibitory antibodies. Oncogene. 2016;35:6077–86.
8. Takebe N, Miele L, Harris PJ, Jeong W, Bando H, Kahn M, et al. Targeting Notch, Hedgehog, and Wnt pathways in cancer stem cells: clinical update. Nat Rev Clin Oncol. 2015;12:445–64.
9. Tsaouli G, Barbarulo A, Vacca A, Screpanti I, Felli MP. Molecular Mechanisms of Notch Signaling in Lymphoid Cell Lineages Development: NF-kappaB and Beyond. Adv Exp Med Biol. 2020;1227:145–64.
10. Radtke F, Fasnacht N, Macdonald HR. Notch signaling in the immune system. Immunity. 2010;32:14–27.
11. Janas ML, Turner M. Stromal cell-derived factor 1alpha and CXCR4: newly defined requirements for efficient thymic beta-selection. Trends Immunol 2010;31:370–6.
12. Tsaouli G, Ferretti E, Bellavia D, Vacca A, Felli MP. Notch/CXCR4 partnership in acute lymphoblastic leukemia progression. J Immunol Res. 2019;2019:5601396.
13. Trampont PC, Tosello-Trampont AC, Shen Y, Duley AK, Sutherland AE, Bender TP, et al. CXCR4 acts as a costimulator during thymic beta-selection. Nat Immunol. 2010;11:162–70.
14. Bellavia D, Campese AF, Alesse E, Vacca A, Felli MP, Balestri A, et al. Constitutive activation of NF-kappaB and T-cell leukemia/lymphoma in Notch3 transgenic mice. EMBO J. 2000;19:3337–48.
15. Felli MP, Vacca A, Calce A, Bellavia D, Campese AF, Grillo R, et al. PKC theta mediates pre-TCR signaling and contributes to Notch3-induced T-cell leukemia. Oncogene. 2005;24:992–1000.
16. Vacca A, Felli MP, Palermo R, Di Mario G, Calce A, Di Giovine M, et al. Notch3 and pre-TCR interaction unveils distinct NF-kappaB pathways in T-cell development and leukemia. EMBO J. 2006;25:1000–8.
17. Franciosa G, Diluvio G, Gaudio FD, Giuli MV, Palermo R, Grazioli P, et al. Prolyl-isomerase Pin1 controls Notch3 protein expression and regulates T-ALL progression. Oncogene. 2016;35:4741–51.
18. Del Gaizo M, Sergio I, Lazzari S, Cialfi S, Pelullo M, Screpanti I, et al. MicroRNAs as modulators of the immune response in T-Cell acute lymphoblastic leukemia. Int J Mol Sci. 2022;23:829.
19. Pitt LA, Tikhonova AN, Hu H, Trimarchi T, King B, Gong Y, et al. CXCL12-producing vascular endothelial niches control acute T Cell leukemia maintenance. Cancer Cell. 2015;27:755–68.
20. Jost TR, Borga C, Radaelli E, Romagnani A, Perruzza L, Omodho L, et al. Role of CXCR4-mediated bone marrow colonization in CNS infiltration by T cell acute lymphoblastic leukemia. J Leukoc Biol. 2016;99:1077–87.
21. Kadakia T, Tai X, Kruhlak M, Wisniewski J, Hwang IY, Roy S, et al. E-protein-regulated expression of CXCR4 adheres preselection thymocytes to the thymic cortex. J Exp Med. 2019;216:1749–61.
22. Maroni P, Bendinelli P, Matteucci E, Desiderio MA. HGF induces CXCR4 and CXCL12-mediated tumor invasion through Ets1 and NF-kappaB. Carcinogenesis. 2007;28:267–79.
23. Wang J, Wang H, Cai J, Du S, Xin B, Wei W, et al. Artemin regulates CXCR4 expression to induce migration and invasion in pancreatic cancer cells through activation of NF-kappaB signaling. Exp Cell Res. 2018;365:12–23.
24. Cheng M, Yang J, Zhao X, Zhang E, Zeng Q, Yu Y, et al. Circulating myocardial microRNAs from infarcted hearts are carried in exosomes and mobilise bone marrow progenitor cells. Nat Commun. 2019;10:959.
25. Alsayed R, Khan AQ, Ahmad F, Ansari AW, Alam MA, Buddenkotte J, et al. Epigenetic regulation of CXCR4 signaling in cancer pathogenesis and progression. Semin Cancer Biol. 2022;86:697–708.
26. Portella L, Bello AM, Scala S. CXCL12 signaling in the tumor microenvironment. Adv Exp Med Biol. 2021;1302:51–70.
27. Dawidowska M, Jaksik R, Drobna M, Szarzynska-Zawadzka B, Kosmalska M, Sedek L, et al. Comprehensive investigation of miRNome identifies Novel Candidate miRNA-mRNA interactions implicated in T-cell acute lymphoblastic leukemia. Neoplasia. 2019;21:294–310.
28. Wallaert A, Van Loocke W, Hernandez L, Taghon T, Speleman F, Van Vlierberghe P. Comprehensive miRNA expression profiling in human T-cell acute lymphoblastic leukemia by small RNA-sequencing. Sc Rep. 2017;7:7901.
29. Bartel DP. MicroRNAs: target recognition and regulatory functions. Cell. 2009;136:215–33.
30. Kumar V, Palermo R, Talora C, Campese AF, Checquolo S, Bellavia D, et al. Notch and NF-kB signaling pathways regulate miR-223/FBXW7 axis in T-cell acute lymphoblastic leukemia. Leukemia. 2014;28:2324–35.
31. Li X, Sanda T, Look AT, Novina CD, von Boehmer H. Repression of tumor suppressor miR-451 is essential for NOTCH1-induced oncogenesis in T-ALL. J Exp Med. 2011;208:663–75.
32. Mansour MR, Sanda T, Lawton LN, Li X, Kreslavsky T, Novina CD, et al. The TAL1 complex targets the FBXW7 tumor suppressor by activating miR-223 in human T cell acute lymphoblastic leukemia. J Exp Med. 2013;210:1545–57.
33. Shu Y, Wang Y, Lv WQ, Peng DY, Li J, Zhang H, et al. ARRB1-Promoted NOTCH1 Degradation Is Suppressed by OncomiR miR-223 in T-cell Acute Lymphoblastic Leukemia. Cancer Res. 2020;80:988–98.
34. Gebarowska K, Mroczek A, Kowalczyk JR, Lejman M. MicroRNA as a prognostic and diagnostic marker in T-cell acute lymphoblastic leukemia. Int J Mol Sci. 2021;22:5317.
35. Rasaiyaah J, Georgiadis C, Preece R, Mock U, Qasim W. TCRalphabeta/CD3 disruption enables CD3-specific antileukemic T cell immunotherapy. JCI Insight. 2018;3:e99442.
36. Yui MA, Rothenberg EV. Developmental gene networks: a triathlon on the course to T cell identity. Nat Rev Immunol. 2014;14:529–45.
37. Dos Santos NR, Ghysdael J, Tran Quang C. The TCR/CD3 complex in leukemogenesis and as a therapeutic target in T-cell acute lymphoblastic leukemia. Adv Biol Regul. 2019;74:100638.
38. Ferrandino F, Bernardini G, Tsaouli G, Grazioli P, Campese AF, Noce C, et al. Intrathymic Notch3 and CXCR4 combinatorial interplay facilitates T-cell leukemia propagation. Oncogene. 2018;37:6285–98.
39. Plotkin J, Prockop SE, Lepique A, Petrie HT. Critical role for CXCR4 signaling in progenitor localization and T cell differentiation in the postnatal thymus. J Immunol. 2003;171:4521–7.
40. Petrie HT, Zuniga-Pflucker JC. Zoned out: functional mapping of stromal signaling microenvironments in the thymus. Annu Rev Immunol. 2007;25:649–79.
41. Coustan-Smith E, Mullighan CG, Onciu M, Behm FG, Raimondi SC, Pei D, et al. Early T-cell precursor leukaemia: a subtype of very high-risk acute lymphoblastic leukaemia. Lancet Oncol. 2009;10:147–56.
42. Shiraz P, Jehangir W, Agrawal V. T-Cell Acute Lymphoblastic Leukemia-Current Concepts in Molecular Biology and Management. Biomedicines. 2021;9:1621.
43. Wallaert A, Durinck K, Taghon T, Van Vlierberghe P, Speleman F. T-ALL and thymocytes: a message of noncoding RNAs. J Hematol Oncol. 2017;10:66.
44. Yi J, Gao ZF. MicroRNA-9-5p promotes angiogenesis but inhibits apoptosis and inflammation of high glucose-induced injury in human umbilical vascular endothelial cells by targeting CXCR4. Int J Biol Macromol. 2019;130:1–9.
45. Qin L, Deng HY, Chen SJ, Wei W, Zhang YT. miR-139 acts as a tumor suppressor in T-cell acute lymphoblastic leukemia by targeting CX chemokine receptor 4. Am J Transl Res. 2017;9:4059–70.
46. Liu Z, Ye P, Wang S, Wu J, Sun Y, Zhang A, et al. MicroRNA-150 protects the heart from injury by inhibiting monocyte accumulation in a mouse model of acute myocardial infarction. Circ Cardiovasc Genet. 2015;8:11–20.
47. Agarwal V, Bell GW, Nam JW, Bartel DP. Predicting effective microRNA target sites in mammalian mRNAs. Elife. 2015;4:e05005.
48. Zhang N, Qu Y, Qin B. Sodium butyrate ameliorates non-alcoholic fatty liver disease by upregulating miR-150 to suppress CXCR4 expression. Clin Exp Pharm Physiol. 2021;48:1125–36.
49. Tano N, Kim HW, Ashraf M. microRNA-150 regulates mobilization and migration of bone marrow-derived mononuclear cells by targeting Cxcr4. PLoS ONE. 2011;6:e23114.

50. He Y, Jiang X, Chen J. The role of miR-150 in normal and malignant hematopoiesis. Oncogene. 2014;33:3887–93.
51. Ghisi M, Corradin A, Basso K, Frasson C, Serafin V, Mukherjee S, et al. Modulation of microRNA expression in human T-cell development: targeting of NOTCH3 by miR-150. Blood. 2011;117:7053–62.
52. Agnusdei V, Minuzzo S, Frasson C, Grassi A, Axelrod F, Satyal S, et al. Therapeutic antibody targeting of Notch1 in T-acute lymphoblastic leukemia xenografts. Leukemia. 2014;28:278–88.
53. Minuzzo S, Agnusdei V, Pinazza M, Amaro AA, Sacchetto V, Pfeffer U, et al. Targeting NOTCH1 in combination with antimetabolite drugs prolongs life span in relapsed pediatric and adult T-acute lymphoblastic leukemia xenografts. Exp Hematol Oncol. 2023;12:76.
54. Gao X, Qin S, Wu Y, Chu C, Jiang B, Johnson RH, et al. Nuclear PFKP promotes CXCR4-dependent infiltration by T cell acute lymphoblastic leukemia. J Clin Investig. 2021;131:e143119.
55. Sciume G, De Angelis G, Benigni G, Ponzetta A, Morrone S, Santoni A, et al. CX3CR1 expression defines 2 KLRG1+ mouse NK-cell subsets with distinct functional properties and positioning in the bone marrow. Blood. 2011;117:4467–75.
56. Ruscher R, Hogquist KA. Intravenous Labeling and Analysis of the Content of Thymic Perivascular Spaces. Bio Protoc. 2018;8:e2757.
57. Martins VC, Busch K, Juraeva D, Blum C, Ludwig C, Rasche V, et al. Cell competition is a tumour suppressor mechanism in the thymus. Nature. 2014;509:465–70.
58. Abdulla HD, Alserihi R, Flensburg C, Abeysekera W, Luo MX, Gray DHD, et al. Overexpression of Lmo2 initiates T-lymphoblastic leukemia via impaired thymocyte competition. J Exp Med. 2023;220:e20212383.
59. Rothenberg EV. Programming for T-lymphocyte fates: modularity and mechanisms. Genes Dev. 2019;33:1117–35.
60. Kyriakidis I, Kyriakidis K, Tsezou A. MicroRNAs and the diagnosis of childhood acute lymphoblastic leukemia: systematic review, meta-analysis and re-analysis with novel small RNA-seq tools. Cancers. 2022;14:3976.
61. Nair RA, Verma VK, Beevi SS, Rawoof A, Alexander LE, Prasad ER, et al. MicroRNA signatures in blood or bone marrow distinguish subtypes of pediatric acute lymphoblastic leukemia. Transl Oncol. 2020;13:100800.
62. Tian XP, Xie D, Huang WJ, Ma SY, Wang L, Liu YH, et al. A gene-expression-based signature predicts survival in adults with T-cell lymphoblastic lymphoma: a multicenter study. Leukemia. 2020;34:2392–404.
63. Tian XP, Huang WJ, Huang HQ, Liu YH, Wang L, Zhang X, et al. Prognostic and predictive value of a microRNA signature in adults with T-cell lymphoblastic lymphoma. Leukemia. 2019;33:2454–65.
64. Abdulla H, Vo A, Shields BJ, Davies TJ, Jackson JT, Alserihi R, et al. T-ALL can evolve to oncogene independence. Leukemia. 2021;35:2205–19.
65. Maroder M, Bellavia D, Vacca A, Felli MP, Screpanti I. The thymus at the crossroad of neuroimmune interactions. Ann N. Y Acad Sci. 2000;917:741–7.
66. Grazioli P, Orlando A, Giordano N, Noce C, Peruzzi G, Abdollahzadeh B, et al. Notch-Signaling Deregulation Induces Myeloid-Derived Suppressor Cells in T-Cell Acute Lymphoblastic Leukemia. Front Immunol. 2022;13:809261.
67. Grazioli P, Felli MP, Screpanti I, Campese AF. The mazy case of Notch and immunoregulatory cells. J Leukoc Biol. 2017;102:361–8.
68. Barbarulo A, Grazioli P, Campese AF, Bellavia D, Di Mario G, Pelullo M, et al. Notch3 and canonical NF-kappaB signaling pathways cooperatively regulate Foxp3 transcription. J Immunol. 2011;186:6199–206.

ACKNOWLEDGEMENTS

The authors wish to acknowledge Ilaria Pia Caporale, Federica Squillante, Noemi Martina Cantale Aeo and Marco Crisci for contribution to the experimental work, Laura Fasano for animal care assistance and the Flow Cytometry Facility at Center for Life Nano-Neuro Science, IIT, for support and technical advice.

AUTHOR CONTRIBUTIONS

IS, CV and SKP designed and performed the experiments, analyzed the data and wrote the first draft of the paper. MDG, AO, FF, and GT performed the experiments. DP, SL, RLS and ZMB analyzed the data. FC, MAV, GB, DDB, ER, SI, SC and SM collaborated on the experiments and analyzed the data. GP did all the sorting experiments. IScre critically revised the manuscript. MPF and AFC supervised the experiments, analyzed the data, and wrote the manuscript. The authors read and approved the final manuscript.

FUNDING

This study was founded by the Sapienza University grants, Avvio alla Ricerca: (AR222181616D9D01) to SKP; Avvio alla Ricerca (AR1181643646B258) to GT; (AR123188AF112A64) to IS; Ateneo 2021 (RP12117A63FBA27C), 2022 (RP122181642E92CE), 2023 (RP123188F3C01EB7) to MPF; Ateneo 2021 (RM12117A71419448) to AFC; MIUR PNR 2015-2020 ARS01_00432, PROGEMA to IScre and by Italian Ministry of Education, University and Research – Dipartimenti di Eccellenza - L. 232/2016; Horizon 2020 (PH118164340087CF) to IScre. The manuscript has been supported by the Croatian Science Foundation grant number HRZZ IP-2020-02-2431(I. Scre and MPF).

COMPETING INTERESTS

The authors declare no conflict of interest.

ETHICS APPROVAL AND CONSENT STATEMENT

RNA samples were obtained from Patient-derived xenografts (PDTALL) after informed consent from all individual participants collected and following the Declaration of Helsinki. All the procedures were approved by the Ethics Committee with the protocol number AIEOP-BFM ALL 2009.

ADDITIONAL INFORMATION

Supplementary information The online version contains supplementary material available at https://doi.org/10.1038/s41388-024-03079-0.

Correspondence and requests for materials should be addressed to Maria Pia Felli.

Reprints and permission information is available at http://www.nature.com/reprints

Publisher's note Springer Nature remains neutral with regard to jurisdictional claims in published maps and institutional affiliations.